Acta Vulcanologica – Vol. 10 (2) – 1998: 339 - 345

Crustal structure of the Rhodope and surrounding area obtained by non-linear inversion of P and S travel times and its tectonic implications

C. B. Papazachos[1], E. M. Skordilis[2]

1. *Institute of Engineering Seismology and Earthquake Engineering, PO Box 53, GR-55102 Foinikas, Thessaloniki, Greece*
2. *Geophysical Laboratory, University of Thessaloniki, PO Box 352-1, GR-54006 Thessaloniki, Greece*

Abstract

The aim of the present study is to present results on the P and S velocity structure of the crust and uppermost mantle in the broader Northern Aegean area with a special emphasis on the results concerning mainly the central and southern part of the Rhodope massif. The velocity structure is derived from the inversion of travel times of local events. An appropriate preconditioning of the final linearized system is used in order to reduce ray density effects on the results. An attempt is made to interpret the features and details of the crustal structure, which can be recognized in the final tomographic images, in terms of the geotectonic setting of the area. The crustal thickness shows strong variations. In contrary to the Serbomacedonian massif, the Rhodope massif does not show a typical thick crust. The crustal thinning of the Northern Aegean Trough (≈25-27 km) extends into the Rhodope massif. In general, the Lower Pangaio Unit of the Rhodope massif exhibits a thinner crust than the Upper Unit or the Serbomacedonian massif, indicating that this is due to the same extensional field which was responsible for its larger uplift, according to recent detachment models (Kilias & Mountrakis, 1998). Moreover, the Rhodope massif is separated from the Serbomacedonian massif by the Strymon river-Orfanou gulf basin, which shows a significant crustal thinning (≈25-28 km) as a result of the same extensional process incident which generated this basin. Crustal thinning rates estimated from the tomographic results agree with denudation rates predicted from the current geological models.

1. Introduction

The Aegean sea (Fig. 1) is one of the seismically most active regions worldwide. In the southern part of the area, the main feature is the subduction of the eastern Mediterranean lithosphere under the Aegean (Papazachos & Comninakis, 1969; McKenzie, 1970, 1978; Le Pichon & Angelier, 1979). The tectonic pattern of the area is fairly typical for a subduction system with shallow events, thrust in the outer arc and normal in the back-arc area (Comninakis, 1975; McKenzie, 1978). On the other hand, a shallow dipping Benioff zone is delineated by the intermediate depth seismicity (Papazachos & Comninakis, 1969, 1971) and a well defined volcanic arc is formed by a number of volcanoes, which coincides with the 150 km isodepth of this Benioff zone. This complicating geotectonic setting as well as the complex evolution of the area has left a strong signature on the geological structure of the area which is reflected in the velocity structure. Refraction experiments (Makris, 1976), travel time studies (Panagiotopoulos & Papazachos, 1985; Papazachos & Nolet, 1997a), and gravity studies (Makris, 1973; Chailas et al., 1992; Papazachos, 1994) show significant variations throughout the whole Aegean lithosphere. The main crustal variations can be explained within the context of the active subduction: The Hellenic Alps which also represent the Hellenic Arc accretionary prism (Fig.1) show a crustal thickenning which locally reaches 45 km. On the other hand, the back-arc area exhibits a much thinner crust of the order of 25-30 km.

Although the eastern Mediterranean subduction explains most of the geological and geophysical features of the southern Aegean, this is not valid for the northern Aegean area. The area is characterized by the presence of Rhodope and the Serbomacedonian metamorphic massives (Mercier, 1968; Kockel et al., 1971) which comprise a mountainous and structurally complex domain of mainly metamorphic rocks and igneous bodies. The two massifs are separated by the Strymon basin which consists of continental sediments with a maximum thickness of the order of 3-4

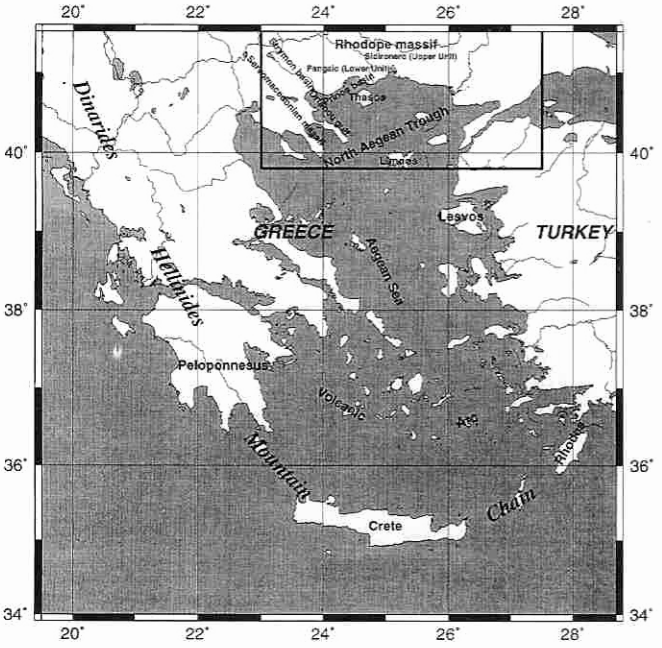

Fig. 1 – General features of the Aegean area. The area under study is delineated by a solid line.

km (Mountrakis,1985). This basin continues to the southeast into the Orfanou gulf. Further to the south both massives are bordered by the North Aegean Trough which represents the continuation of the North Anatolian Fault in the North Aegean.

Although the Serbomacedonian massif and the North Aegean Trough exhibit a high seismicity (e.g. Scordilis, 1985), this is not true for the Rhodope massif. The general earthquake pattern corresponds to mainly dextral strike-slip and normal faults with occasional dextral strike-slip component (e.g. Papazachos, 1990), as a result of the strike-slip deformation along the North Aegean Trough and the NNW-SSE back-arc extension, respectively (Papazachos et al., 1993). However, this last recent extensional field is not as evident as the older NE-SW extensional field which has a dominant signature throughout the whole Rhodope massif. Recent studies suggest that this field might be dated back to Cretaceous-Early Tertiary times (Kilias et al., 1995).The result of this field and the associated detachment system responsible for the creation of the NW-SE trending basins of the area (Axios basin, Strymon basin, Drama basin, etc.) has been recently discussed to a large extent by various reasearchers (Dinter & Royden, 1993; Sokoutis et al., 1993; Dinter et al., 1995; Kilias & Mountrakis, 1998).

In the present paper, the detailed characteristics of the velocity structure of the broader northernmost Aegean region is studied, with an emphasis in the Rhodope area. The Serbomacedonian massif has been extensively studied in a previous study (Papazachos, 1998). The main modification to the standard tomographic approach is the use of a modified inversion technique (Papazachos & Nolet, 1997b) which incorporates 3-D ray tracing. S waves are also included in the present study. We mainly focus on the Rhodope massif, its contacts with the Serbomacedonian massif and the North Aegean Trough. A large data set of more than 60,000 P and S travel times is employed from 4352 local events for the time period 1981-1995. An appropriate preconditioning of the final linear system, using a crude estimate of the *a posteriori* covariance matrix is applied, in order to correct for ray density effects on our results. New information concerning the structure of the area can be recognized in the final results. An attempt is made to interpret the tomographic results in terms of the geotectonic structure of the area.

2. Travel time data

The area under study is delineated with the thick solid line in figure (1). The main source of travel-time data is the annual and monthly bulletins of the Geophysical Laboratory of the University of Thessaloniki (GLUT) for the time period 1981-1995. An additional section of the data set came from the monthly bulletins of seismological observatories of Greece and neighbouring countries. All events are relocated by the GLUT using an appropriate local model for the Serbomacedonian massif (Scordilis, 1985) extended to the Rhodope by the results of a larger scale tomographic study (Papazachos et al., 1995). During the relocation process, travel times were checked for outliers. Moreover, we included data collected from a local seismicity monitoring network located in the Nestos river area.

A typical problem in local studies is the «contamination» of the results due to the presence of mislocated earthquakes. Therefore, certain criteria were established for the data selection based on the results of a previous analysis of earthquake locations for Greece (Karakostas, 1988). Hence, only events with at least 9 P and 1 S phases were used. Moreover, phases reported as impulsive were assigned a higher weight (typically a factor of 2). The final data set consists of ≈38,500 P and 21,000 S arrivals, recorded at 35 permanent and 5 temporary stations. The final epicenters, of the events for which data were used, and the station locations are depicted in figure 2, where the area under study is delineated by a thick solid line.

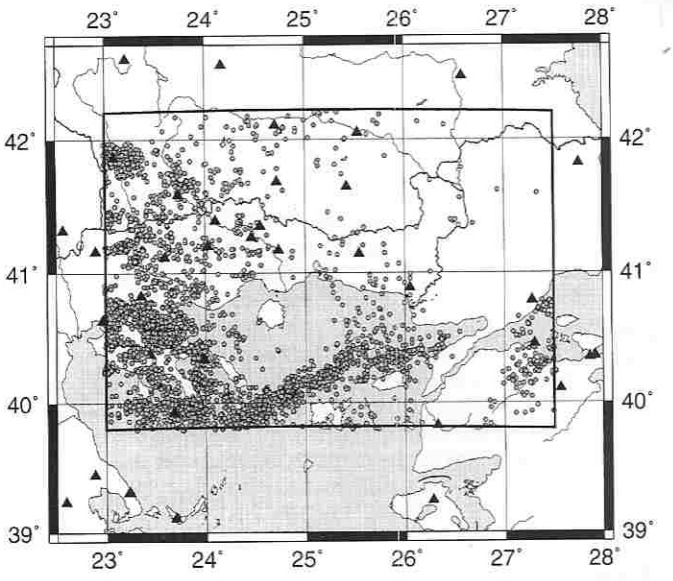

Fig. 2 – Map of the epicenters (denoted with circles) of the events for which data were used in the present study. Permanent and temporary stations are depicted by solid triangles.

3. Travel time inversion

The target of the travel-time of local earthquakes is to simultaneously determine the velocity structure and relocate the earthquakes in the new 3-D velocity medium (Aki & Lee, 1976). The travel time residual is expressed as a function of the perturbations of the event's hypocentral parameters and the velocity model, which is linearized using an initial approximate solution (e.g. derived from 1-D ray theory). Finally, a system of equations of the following form can be defined:

$$\mathbf{d} = \mathbf{B}\,\mathbf{h} + \mathbf{C}\,\mathbf{v} + \mathbf{c} \qquad (1)$$

where **d** contains the travel time residuals, **B** and **C** are the hypocentral and velocity derivative matrices, **h** and **v** are the hypocentral and velocity corrections vectors. A station correction vector, **c**, is also included in order to account for anything that can not be explained by the retrieved velocity structure (e.g. local structure beneath a station, systematic time shifts at a station, etc.). Clearly, equation (1) can be concatenated into:

$$\mathbf{d} = \mathbf{A}\,\mathbf{x} \qquad (2)$$

where **A** and **x** simply combine matrices **B**, **C** and **I**(identity matrix) and vectors **h**, **v** and **c**, respectively. In the present

study a trilinear interpolation function was chosen for the model representation (Thurber, 1983). This choice imposes that the problem must be treated as a mixed-determined problem. Hence, a «least-structure» solution (Franklin, 1970; Tarantola & Nercessian, 1984; Constable et al., 1987) is constructed by considering additional constraints and minimizing the model or the model second derivative norms. In the present study equation (2) is modified (Papazachos & Nolet, 1997a), as follows:

$$\mathbf{C_d^{-1/2} A\, C_x^{1/2} S\, H\, z = C_d^{-1/2} d}$$
$$\boldsymbol{\lambda}\, \mathbf{I\, z = 0} \qquad (3)$$

where $\mathbf{C_d}$ is the data covariance matrix, $\mathbf{C_x}$ is the *a priori* estimate of the model covariance matrix (usually diagonal), **S** is an appropriate smoothing matrix (e.g.Spakman & Nolet, 1988) and $\boldsymbol{\lambda}$ is a constant which regulates the strength of our additional minimum norm (damping) constraints. Here, an additional diagonal scaling matrix of the form $\mathbf{H}=\mathrm{diag}\{h_j^{-1/2}\}$ is included, where h_j is a measure of the jth column length of the matrix $\mathbf{A'}= \mathbf{C_d^{-1/2} A\, C_x^{1/2} S}$. In this approach, $\mathbf{x^T C_x^P x}$ is minimized, instead of the usual $\mathbf{x^T C_x\, x}$., where $(\mathbf{C_x^P})^{1/2} = \mathbf{C_x^{1/2} S\, H}$ is our preliminary estimate of the square root of the *a posteriori* model covariance matrix, in an attempt to reduce relative errors in the final solution. Therefore, we partly anneal the correlation that is observed between areas of high ray density (large column length of matrix **A'**) and strong velocity perturbations (Papazachos & Nolet, 1997a)

Our velocity model consists of a rectangular grid of nodes where the slowness is defined. At every point the slowness is calculated by trilinear interpolation of the 8 neighbouring nodes' velocity values. In our case, the grid consisted of 17850 P and S velocity nodes with a horizontal and vertical grid spacing which was set to 20 km and 3 km, respectively. This specific selection of grid spacing was imposed by the amount of available data and corresponds to the maximum resolution that could be achieved due to the poor ray coverage of some areas. The initial velocity values were determined using a typical Herglotz-Wiechert 1-D inversion. A cut-off residual of 2.5 sec was adopted from previous studies (e.g Papazachos, 1998) in order to eliminate the effect of outliers. Moreover, based on previous results (e.g. Scordilis, 1985; Karakostas, 1988; Ligdas & Lees, 1993) appropriate values were determined for the variance of the P and S slowness perturbation norms as well as for the hypocentral station corrections.

A large set of values were tried for the damping coefficients, $\boldsymbol{\lambda}$, and the value of $\boldsymbol{\lambda}$=1.5 was finally adopted which is larger than the theoretical value (e.g.Franklin, 1970). The necessity of a larger value in our case is shown in figure (3) where the P and S residual distribution, before and after the inversion are shown, respectively. It is clear that the residual distribution is not completely Gaussian, even after the inversion. Therefore, a higher damping value is necessary in order to obtain a robust solution which will be relatively unaffected to the larger number of outliers in the real residual distribution. Equation (2) was solved with LSQR (Paige & Saunders, 1982) which has been shown to have superior converging properties. After each LSQR iteration **A** was recomputed using a revised 3-D bending ray tracing algorithm (Moser et al., 1992) and the new linear system was solved again with LSQR. This procedure was repeated 3 times until no significant misfit

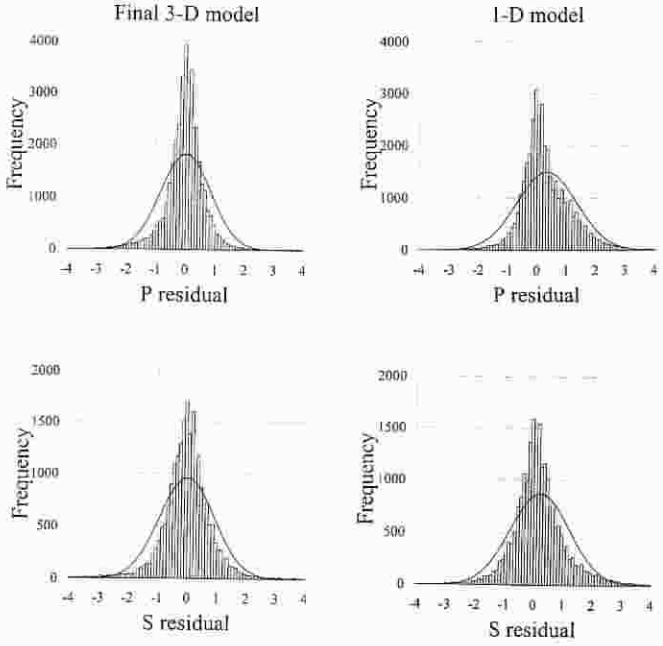

Fig. 3 – Plot of the P and S residual distribution, before (right) and after (left) inversion. Although, the residuals distribution is significantly improved in the final results, it is quite different from Gaussian.

change was observed using LSQR, without an extreme model norm increase. Between succesive iterations a misfit increase was observed, due to the non-linearity of the problem (e.g. Tarantola, 1987), in accordance with recent tomographic studies and synthetic tests (Sambridge, 1990; Papazachos & Nolet, 1997b). The initial and final weighted combined (P and S) rms misfit for the inversion correspond to 0.81s to 0.63s, respectively.

4. Tomographic results

Figures 4 and 5 show the final P and S velocity distribution for different depths which focus at the upper crustal (6-10km) and lower crustal-upper mantle (26-38km) layers. In both figures, results are not shown for the areas which are poorly sampled by the data. An impressive contrast is observed in the shallow layers for both the P and S velocities: although the Serbomacedonian massif is delineated as a NW-SE trending zone of strong negative velocity perturbations, the Rhodope area shows a completely different behaviour, with significantly higher velocities. Therefore, although the two massives were exposed to extensive deformation, the metamorphic basement seems to be deforming significantly faster for the Rhodope massif. A probable explanation is that, at least the central-southwestern part (see the velocity distribution at 10km) of the Rhodope massif, was originated from lower crustal areas than the Serbomacedonian massif. This observation is expected since this area is dominated by the Lower Rhodope Unit which is a relatively lower crustal formation than the Serbomacedonian massif, as it is also indicated by the recently proposed detachment between the two massives (Dinter & Royden, 1993; Sokoutis et al., 1993).

The situation is similar for the deeper part of the crust and the uppermost mantle for the southern central part of the Rhodope massif, with high velocities clearly indica-

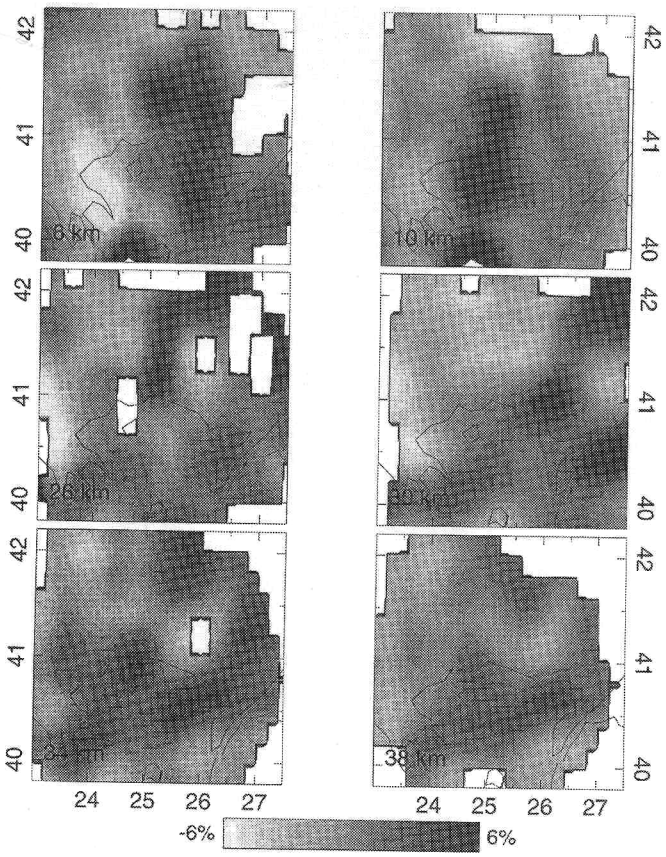

Fig. 4 – P velocity perturbations for the final 3-D model.

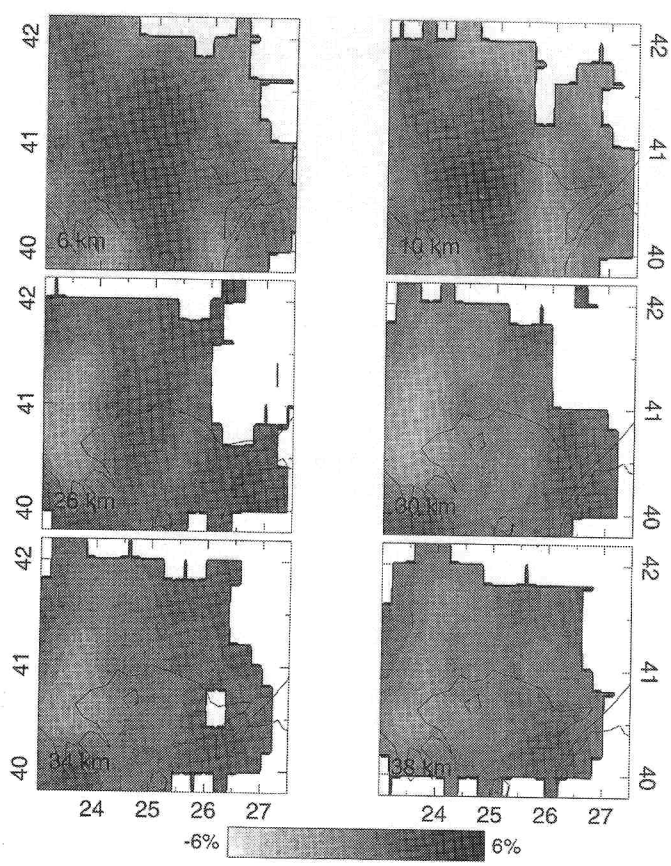

Fig. 5 – Same as figure 4 for the S velocities.

tive of the crustal thinning of the area. On the contrary, the northern part of Rhodope gradually develops lower velocities. A well known W-SW to E-NE zone of positive anomalies (crustal thinning) is observed along the North Aegean Trough, in agreement with earlier tomographic (Papazachos et al., 1995, Papazachos, 1998), travel time (Panagiotopoulos & Papazachos, 1985) and gravity studies (Brooks & Kiriakidis, 1986). This zone seems to extend towards the Thassos island and the Lower Pangaio Unit. At the same time, the two massives are separated by a NW-SE trending zone of positive velocity perturbations, which corresponds to the Strymon basin, clearly seen at the depths of 26 and 30 km. These perturbations can be attributed to a crustal thinning in these area. The S velocities exhibit a quite good consistency with the corresponding P results, although the resolution is relatively poorer.

5. Discussion and conclusions

In figure 6 the P velocity distribution is plotted along three cross-sections of the area. Since in the present study only direct and transmitted (head) waves were used, it is difficult to infer accurate information about the Moho depth. Therefore, the velocity scale is separated in two areas which represent crustal and upper mantle velocities, in such a way that the Moho discontinuity is approximately delineated. The first profile is perpendicular to the main axis of the Serbomacedonian massif. The massif is clearly recognized as a bulk of low velocities which is thickening in the center of the belt (up to 36-37 km) and thinning towards its edges. Under the Strymon basin the crust is thinning to less than 30 km and high velocities are observed in the overlying crustal layers. This pattern is probably a result of the same extensional field which is responsible for the creation of this basin. As we move towards the NW Rhodope (Sidironero-Upper Unit) the crust is thickening and obtains typical but not thick crust (32-34 km).

The second profile shows similar strong crustal thickness variations. As we move to the north from the typical crust of NW Asia Minor ($\simeq$33 km), we have a strong thinning under the North Aegean Trough which remains constant and possibly increases under the Thassos island and the Pangaio area (Lower Unit), with a crustal thickness which is locally less than 25 km. Further north the crust again obtains normal values. The last profile runs accross the examined area. Again we observe the crustal thinning to the west of the Serbomacedonian massif, towards the Orfanou gulf-Prinos basin-Thassos island, reaching a minimum crustal thickness around 25 km. As we enter the mainland further to the E-NE, towards the southern part of Upper Rhodope Unit, we abruptly find a thicker crust ($\simeq$35 km).

The observed crustal structure is especially interesting in connection with the geotectonic setting of the area. The Rhodope massif shows very different characteristics than its neighbouring Serbomacedonian massif. This study, in accordance with previous results (Papazachos, 1998), shows that the Serbomacedonian massif behaves as a NW-SE trending uniform thick block (maximum Moho depth $\simeq$38km), bounded by similarly trending basins which are underlied by a thin crust. Is has been established that both the Strymon and the Axios basins have assumed there present NW-SE dominant elongation due to the Miocene-Pliocene NE-SW extensional field (Mountrakis, 1985).

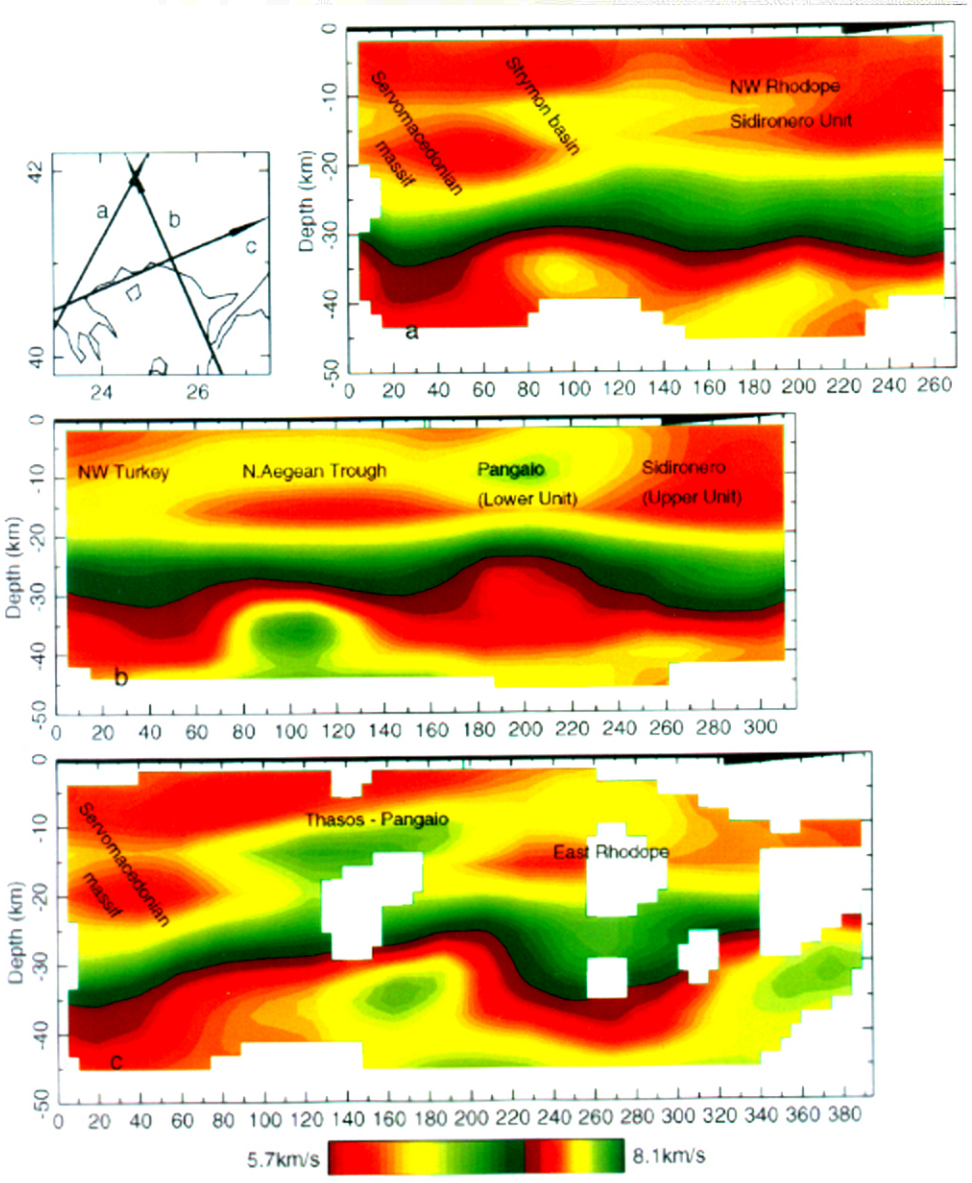

Fig. 6 – P velocity distribution along the three cross-sections in the studied area. The position of the various geologic units has been noted on the profiles. Notice the strong crustal thinning in the Strymon basin-Pangaio-Thasos area shown in all cross-sections.

Recent datings for the Strymon basin place the initiation of the main face of this extension in early Miocene (Dinter et al., 1995), although there are indications that this field is present since Cretaceous (Kilias et al., 1995).

On the other hand, the Rhodope massif does not exhibit this uniform pattern, but seems to be «broken» by the same extensional field which is responsible for the high degree metamorphism (isotherm raising, high heat flow), migmatization and magmatism observed throughout the whole Rhodope (e.g. Kilias & Mountrakis, 1998). The same field is responsible for the crustal thinning of the area, as well as the generation of the various Rhodope basins (Strymon, Drama, Nestos, etc.). The Upper Rhodope Unit (Sidironero) seems to have a typical crustal thickness (≃33-35 km). However, the Pangaio formation (Lower Unit) as well as the Thasos island area seem to have a much thinner crust, reaching locally values smaller than 25 km. This observation indicates stronger extention, crustal thinning and uplift of the area, hence a deeper crustal origin for this Unit. This is in agreement with recent models (Kilias & Mountrakis, 1998) that the broader Pangaio Unit has been uplifted since Miocene to its present position between the Serbomacedonian and Upper Rhodope (Sidironero) Unit.

It is difficult to associate this thinning with the similar situation which holds in the North Aegean Trough, especially since there are still controversial results about the age of the dextral motion along the Trough which range from Oligocene (Kilias & Mountrakis, 1998) to Miocene (e.g. Lyberis, 1984) and up to late Pliocene (Dinter & Royden, 1993). In any case, Rhodope does not exhibit the typical characteristics of a thick-crust metamorphic block. The extensional field since Oligocene has resulted in a significant overall thinning of the area, clearly indicated in the tomographic results. It must be noted that the results presented in the present work are probably a smooth version of the true crustal thickness variations due to the damping which is incorporated in the inversion of the travel-time data (equation 3). Hence, the observed crustal thickness

contrast of ≃10 km between e.g. the Serbomacedonian massif and the Pangaio Unit is probably a low limit of the true contrast. The assumption that this thinning was created by a constant extensive deformation from late Oligocene-uppermost Miocene up to late Pliocene, results in a vertical strain rate, $\dot{\varepsilon}_z$, of the order of $1\text{-}1.5*10^{-8}$/yr, which corresponds to approximately a crustal thinning of the order 0.35-0.5 mm/yr. This thinning followed the initial thinning of the region after the Eocene collisional tectonics in the area until early Miocene (Kilias & Mountrakis, 1998). If we accept a typical value of 43-45 km, observed today in the accretionary prism (e.g. Papazachos & Nolet, 1997a) for the starting thickness of the area, we find a slightly smaller thinning rate of the order of 0.25-0.3 mm/yr for the Serbomacedonian massif, until Early Miocene. Based on depth-pressure results, Kilias et al. (1995) deduced a similar value for the denudation rate of the Serbomacedonian massif for the time interval up to Early Miocene.

It is interesting to notice that present day deformation rates, mainly for the North Aegean Trough, are significantly larger ($\dot{\varepsilon}_z=6\text{-}25*10^{-8}$/yr, Papazachos & Kiratzi, 1996). Although this indicates that the crustal thickness contrasts might have been underestimated, it is more probable to assume that the deformation rate has not been constant during the Miocene-Pliocene deformation period, or even earlier. Therefore, unless a severe change of the deformation regime has occured at late Pliocene, the extention must have taken place in small time intervals, when the deformation was much more intense than its average backround value.

Acknowledgments

The author would like to thank Prof. B.C. Papazachos for carefully reading the manuscript and for his fruitful suggestions. This research has partly been funded by the EEC project EV5V-CT93-0281.

REFERENCES

Aki, K. & Lee, W. H. K. (1976): Determination of three-dimensional velocity anomalies under a seismic array using first P arrival times from local earthquakes: 1.A homogeneous initial model. J. Geophys. Res., 81, 4381-4399

Brooks, M. & Kiriakidis, L. (1986): Subsidence of the north Aegean trough: an alternative view. J. Geol. Soc. London, 143, 23-27.

Chailas, S., Hipkin, R.G. & Lagios, E. (1992): Isostatic studies in the Hellenides. 6th Congr. Geol. Soc. Greece Proc., 25-27 May, Athens.

Comninakis, P. E. (1975): A contribution to the investigation of the seismicity of the area of Greece. Ph.D. Thesis, University of Athens, 110pp. (in Greek).

Constable, S. C., Parker, R. L. & Constable, C. (1987): Occam's inversion: A practical algorithm for generating smooth models from electromagnetic sounding data. Geophysics, 52, 289-300.

Dinter, D. A. & Royden, L. (1993): Late Cenozoic extension in northeastern Greece: Strymon Valley detachment system and Rhodope metamorphic core complex. Geology, 21, 45-48.

Dinter, D. A., Macfarlane, A., Hames, W., Isachsen, C., Bowring, S. & Royden, L. (1995): U-Pb and $^{40}Ar/^{39}Ar$ geochronology of the Symvolon granodiorite: Implications for the thermal and the structural evolution of the Rhodope metamorphic core complex, northeastern Greece. Tectonics, 14, 886-908.

Franklin, J.N. (1970): Well-posed stochastic extension of ill-posed linear problems. J. Math. Anal. Appl., 31, 682-716.

Karacostas, B. (1988): Relation between the seismic activity and geological and geomorphological features of the Aegean and surrounding area. Ph.D. Thesis, University of Thessaloniki, 243pp., (in Greek).

Kilias, A., Falalakis, G. & Mountrakis, D. (1995): Alpine structures and kinematics of the Serbomacedonian metamorphic rocks related to the uplifting of the Hellenic hinterland (Macedonia, Greece). Academy of Athens Proc., 1995.

Kilias, A.A. & Mountrakis, D.M. (1998): Tertiary extension of the Rhodope massif associated with granite emplacement (Northern Greece). Acta Vulcanologica, this volume.

Kockel, F., Mollat, H. & Walther, H. (1971): Geologie des Serbo-Mazedonischen Massivs und seines mesozoichen Rahments (Nord-Griechland). Geol. Jb., 89, 529-551.

Le Pichon, X. & Angelier, J. (1979): The Hellenic arc and trench system: a key to the neotectonic evolution of the eastern Mediterranean area. Tectonophysics, 60, 1-42.

Ligdas, C. N. & Lees, J. M.(1993): Seismic velocity constrains in the Thessaloniki and Chalkidiki areas (northern Greece) from a 3-D tomographic study. Tectonophysics, 228, 97-121.

Lyberis, N. (1984): Tectonic evolution of the North Aegean Trough. In: «The geological evolution of Eastern Mediterranean», J. E. Dixon, & A. H. F. Robertson (Eds.), Geol. Soc. London, Special Publ., 17, 709-725.

Makris, J. (1973): Some geophysical aspects of the evolution of the Hellenides. Bull. Geol. Soc. Greece, 10, 206-213.

Makris, J. (1976): A dynamic model of the Hellenic arc deduced from geophysical data. Tectonophysics, 36, 339-346.

Mercier, J. (1968): Etude géologique des zone internes des Hellenides en Macedoine centrale. Ann. Géol. Pays. Hell., 20, 1-735.

McKenzie, D. P. (1970): The plate tectonics of the Mediterranean region. Nature, 226, 239-243.

McKenzie, D. P. (1978): Active tectonics of the Alpine-Himalayan belt: the Aegean sea and surrounding regions. Geophys. J. R. astr. Soc., 55, 217-254.

Moser, T. J., Nolet, G. & Snieder, G. (1992): Ray bending revisited. Bull. Seism. Soc. Am., 82, 259-289.

Mountrakis, D. M. (1985): Geology of Greece. Univ. Studio Press, Thessaloniki, (in Greek).

Paige, C. C. & Saunders, M. A. (1982): LSQR: An algorithm for sparse linear equations and sparse least squares. A.C.M. Trans. Math. Softw., 8, 43-71.

Panagiotopoulos, D. G. & Papazachos, B. C. (1985): Travel times of P_n-waves in the Aegean and surrounding area. Geophys. J. R. astr. Soc., 80, 165-176.

Papazachos, B. C. (1990): Seismicity of the Aegean and the surrounding area, Tectonophysics, 178, 287-308.

Papazachos, B. C. & Comninakis, P. E. (1969): Geophysical features of the Greek Islands Arc and Eastern Mediterranean Ridge. Comp. Rend. des Seances de la Conference Reunie a Madrid, 16, 74-75.

Papazachos, B.C. & Comninakis, P. E. (1971): Geophysical and tectonic features of the Aegean arc. J. Geophys. Res., 76, 8517-8533.

Papazachos, C. B. (1994): Structure of the crust and upper mantle in SE Europe by inversion of seismic and gravimetric data. Ph.D Thesis, University of Thessaloniki, 208pp., (in Greek).

Papazachos, C. B. (1998): Crustal and upper mantle P and S velocity structure of the Serbomacedonian massif (Northern Greece). Geophys. J. Letters, 134, 25-39.

Papazachos, C. B. & Nolet, G. (1997a): P and S deep velocity structure of the Hellenic area obtained by robust non-linear inversion of arrival times. J. Geophys. Res., 102, 8349-8367.

Papazachos, C. B. & G., Nolet (1997b): Non-linear arrival time tomography. Ann. Geofis., 40, 85-97.

Papazachos, C. B., Kiratzi, A. A. & Papazachos, B. C. (1993): Rates of active crustal deformation in the Aegean and the surrounding area. J. Geodynamics, 16, 147-179.

Papazachos, C. B. & Kiratzi, A. (1996): A detailed study of the active crustal deformation in the Aegean and surrounding area, Tectonophysics, 253, 129-154.

Papazachos, C. B., Hatzidimitriou, P. M., Panagiotopoulos, D. G. & Tsokas, G. N. (1995): Tomography of the crust and upper mantle in southeast Europe. J. Geophys. Res., 100, 12,405-12,422.

Sambridge, M. S. (1990): Non-linear arrival time inversion: constraining velocity anomalies by seeking smooth models in 3-D. Geophys. J. Int., 101, 157-168.

Scordilis, E. M. (1985): Microseismic study of the Serbomacedonian zone and the surrounding area. Ph.D. Thesis, University of Thessaloniki, (in Greek), 250pp..

Sokoutis, D., Brun, J. P., Van den Driessche, J. & Pavlides, S. (1993): A major Oligo-Miocene detachment in southern Rhodope controlling north Aegean extension. J. Geol. Soc. London, 150, 243-246.

Spakman, W. & Nolet, G. (1988): Imaging algorithms, accuracy and resolution in delay time tomography. In: «Mathematical Geophysics», N. J. Vlarr, G. Nolet, M. J. R. Wortel & S. A. P. L. Cloetingh (Eds.), Reidel, Dordrecht, 155-187.

Tarantola, A. (1987): Inverse problem theory. Elsevier, Amsterdam, 613 pp.

Tarantola, A. & Nercessian, A. (1984): Three-dimensional inversion without blocks. Geophys. J. R. astr. Soc., 79, 299-306.

Thurber, C. H. (1983): Earthquake locations and three-dimensional crustal structure in the Coyote Lake area, central California. J. Geophys. Res., 88, 8226-8236.

Received October 1996
Revised MS accepted August 1997